Supplementary Material: Evidence accumulation detected in BOLD signal using slow perceptual decision making

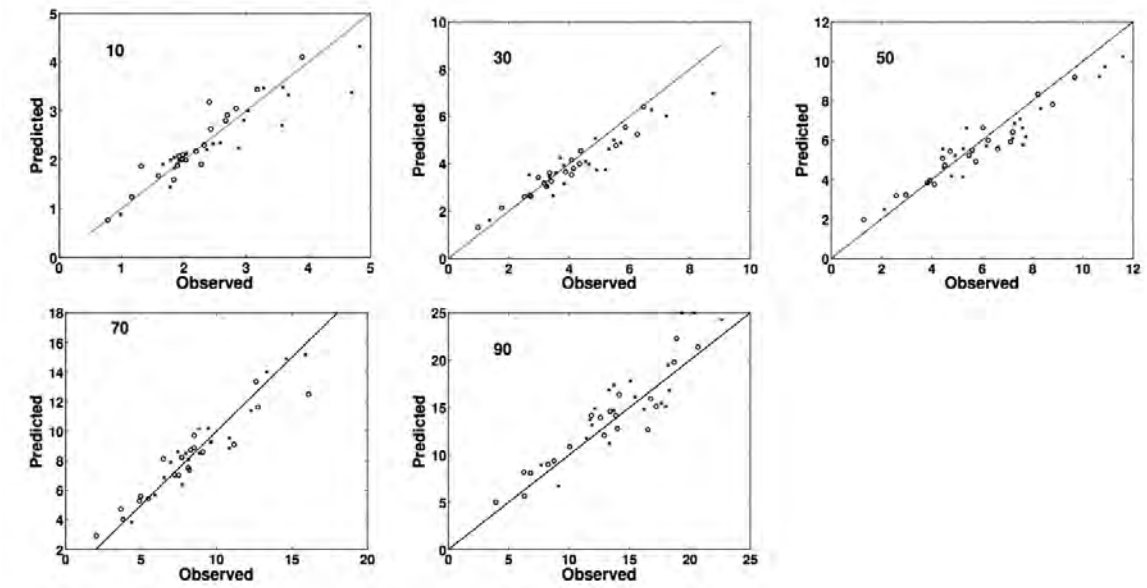

Fig. S1. Quality of the Drift Diffusion Model fit. For each quantile of the response time (RT) distribution, the RT predicted by the model is plotted as a function of the observed RT. Each point represents data from one participant for low coherence trials ('x') and high coherence trials ('o'). Diagonal lines show points of equality between predicted and observed RTs. A perfect fit would have all points on the diagonal line.

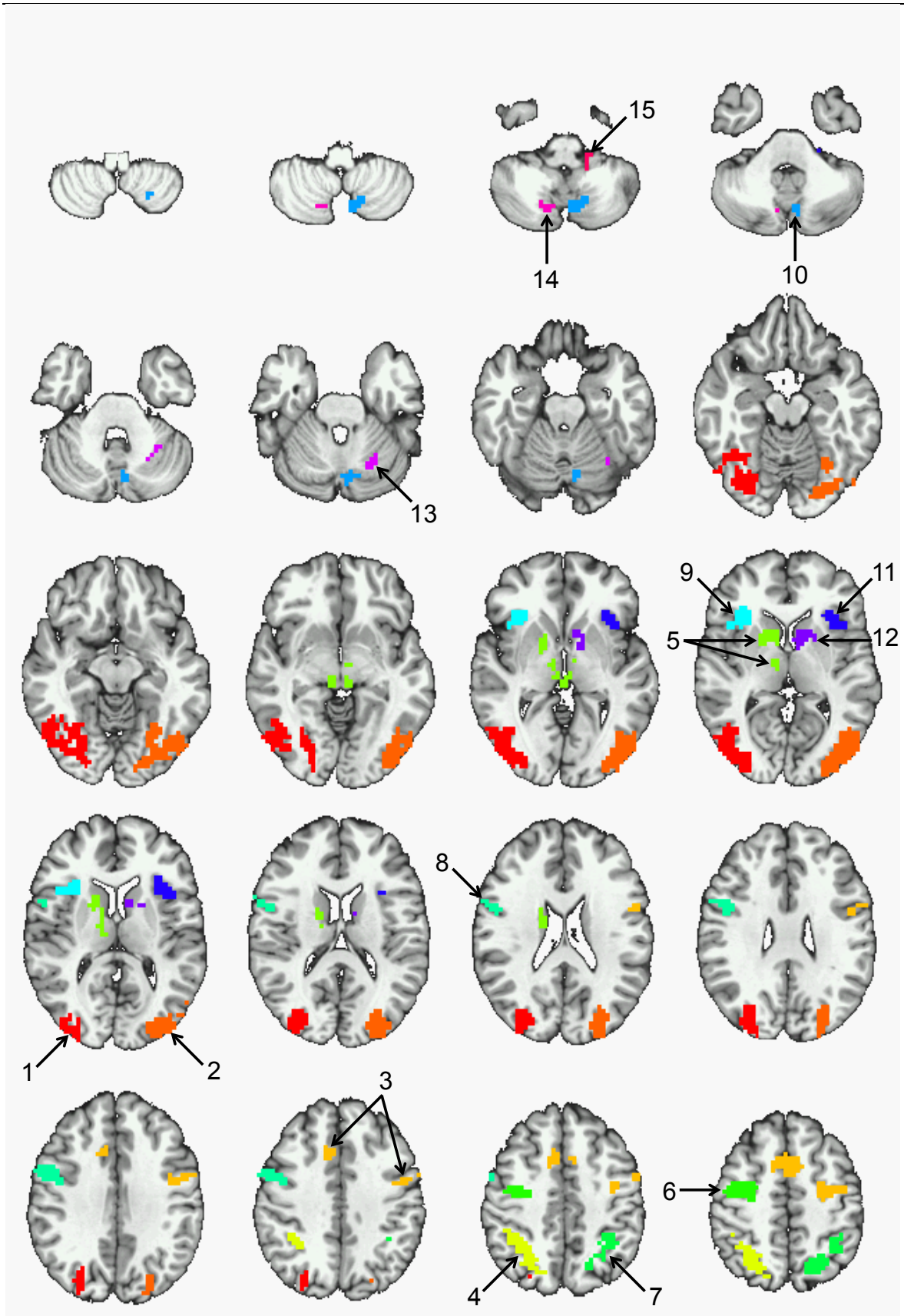
15
14
10
13
9
11
5
12
8
1
2
3
4
7
6

Fig. S2. Areas showing greater activation for dots trials than for arrows trials, irrespective of ramping activity. Numbers indicate separate clusters, ordered by size, the parameter estimates of which are shown in Figs. S3 and S4. (Images are shown in the radiological view, with the left side of each image corresponding to the right side of the head, and with a five-slice gap between subsequent anatomical slices).

	Name	Voxels	X	Y	Z
1	R middle occipital gyrus / BA 19	625	-35.3	72.5	5.9
2	L middle occipital gyrus / BA 19	576	33.8	75.8	5.8
3	L frontal eye fields + L premotor + medial frontal gyrus	363	18.5	0.2	46.2
4	R superior + inferior parietal lobule / BA7	193	-27.9	56.0	45.8
5	R caudate + red nucleus	155	-8.0	9.7	5.2
6	R premotor	144	-34.0	9.5	50.2
7	L superior + inferior parietal lobule / BA7	126	27.0	56.0	47.0
8	R frontal eye fields	120	-49.4	-2.6	29.5
9	R anterior insula	90	-34.6	-19.0	7.0
10	L cerebellum (inferior semi-lunar lobule)	87	10.2	64.8	-34.3
11	L anterior insula	86	32.8	-17.7	8.8
12	L caudate	50	11.2	-5.6	7.3
13	L cerebellum (culmen)	21	26.0	56.0	-23.2
14	R cerebellum (inferior semi-lunar lobule)	16	-11.4	65.3	-38.5
15	L anterior cerebellum	11	18.4	30.1	-37.7

Table S1. Areas showing a main effect of trial type (dots vs. arrows).

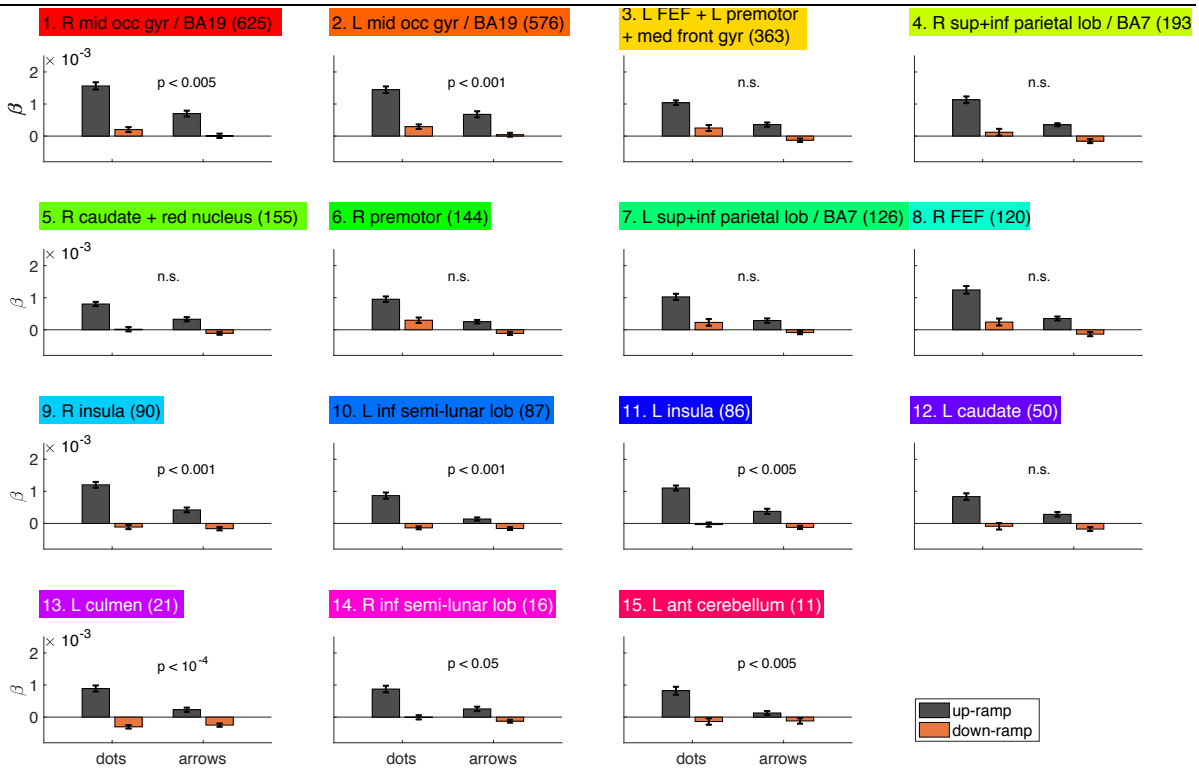

Fig. S3. Parameter estimates (beta-weights) for dots vs. arrows trials and up-ramp vs. down-ramp regressors. Each subplot shows the average beta-weight for a given cluster in Fig. S2, averaged across all participants with error-bars indicating the standard error of the mean. The number in parentheses indicates the number of voxels in a given cluster (cf. Table S1). P-values indicate the Bonferroni-corrected significance of the t-test on the interaction between trial type (dots vs. arrows) and regressor type (up-ramp vs. down-ramp).

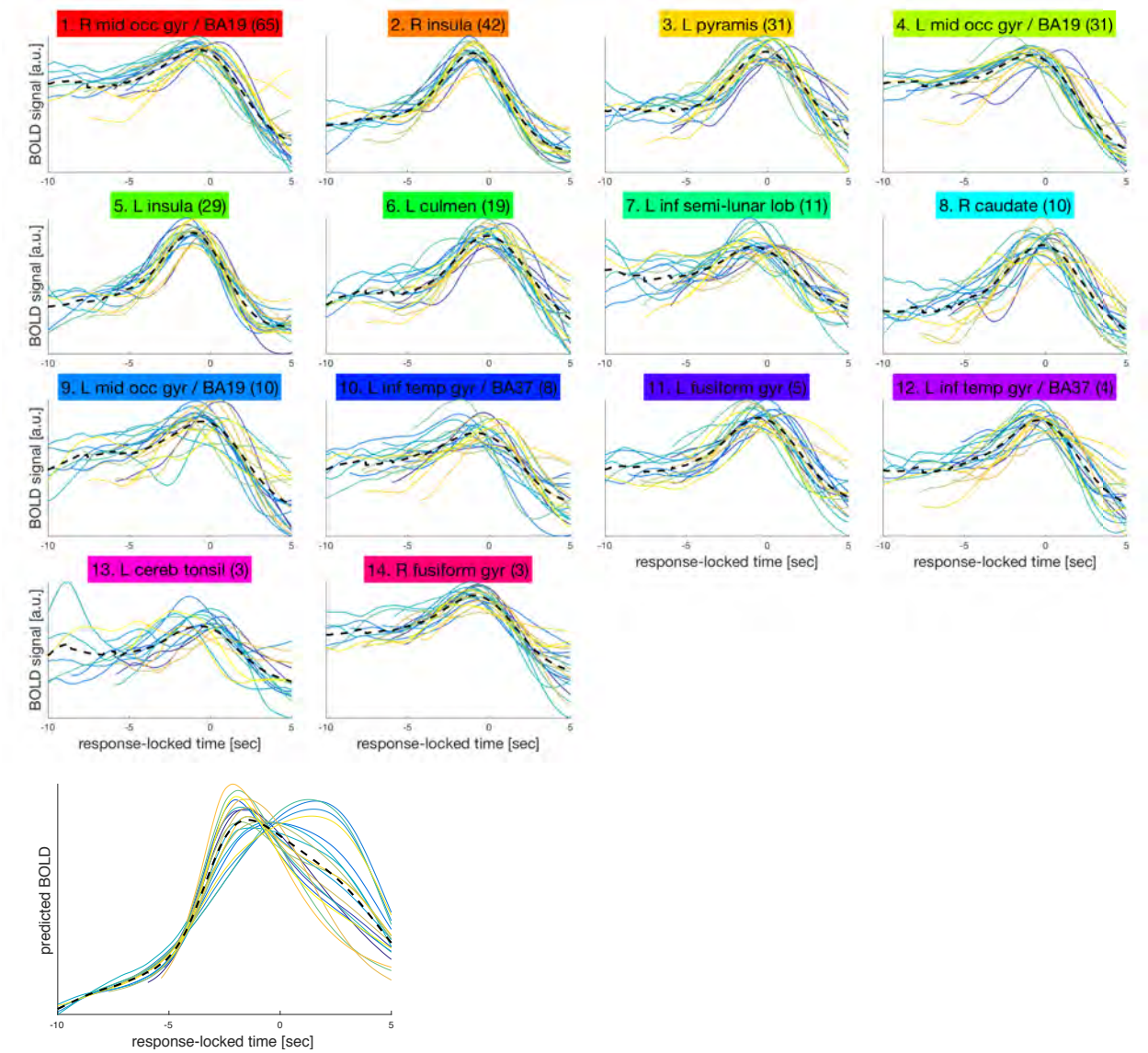

Fig. S4. Response-locked timeseries data from each ROI. Each solid curve shows the BOLD activity averaged across dots trials for a single subject, within a given ROI. The dashed black curve shows the group average. Each participant's curve begins based on their mean RT, to avoid averaging a small number of trials (this can be seen for participants with a mean RT less than 10). The figure on the bottom shows what the timeseries would look like if the signal matched the up-ramp regressors perfectly. This shows an apparent curvature to the ramping signal which is due to averaging across trials of different lengths (not due to a non-linear underlying accumulation signal).

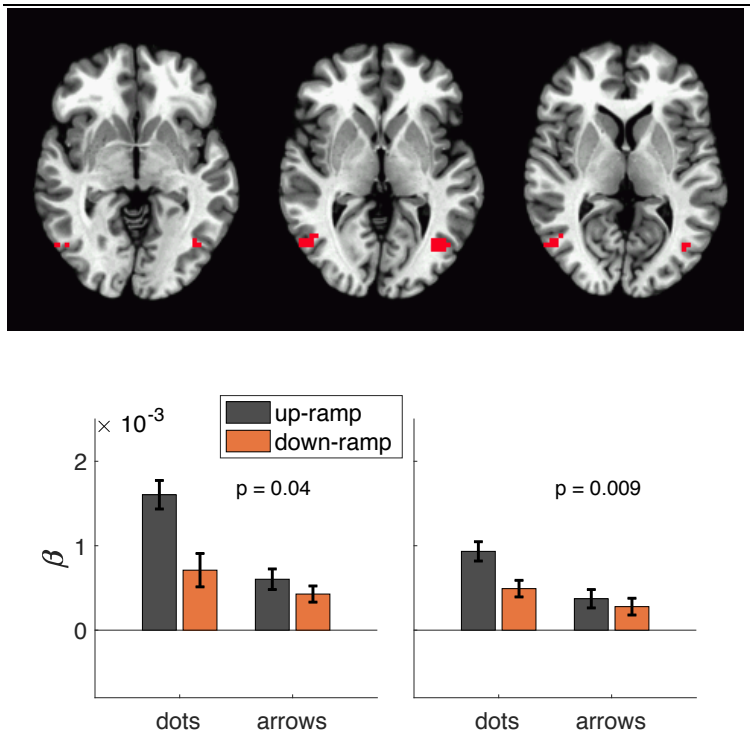

Fig. S5. Although none of the areas involved in evidence accumulation (Figs. 8-9) include area MT, there is partial overlap between areas with significantly greater activation in the dots trials than in the arrows trials (Figs. S2-S3) and area MT. This figure illustrates an anatomically-defined area MT (as defined using the MNI atlas), and the beta-weights within these regions. P-values indicate the uncorrected significance of the interaction between trial type (dots vs. arrows) and regressor type (up-ramp vs. down-ramp). (Images are shown in the radiological view, with the left side of each image corresponding to the right side of the head, and with a four-slice gap between subsequent anatomical slices).

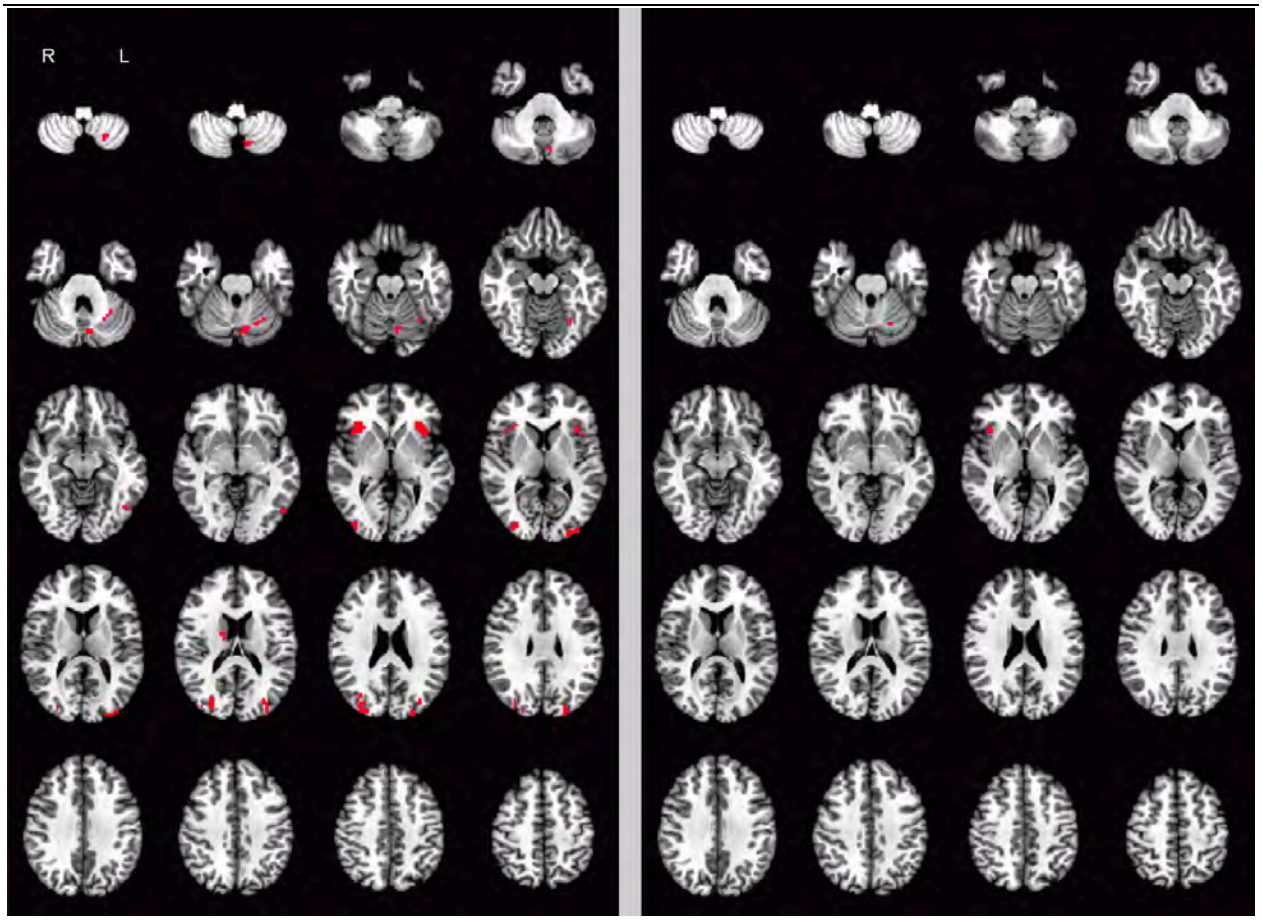

Fig. S6. Results when using a boxcar regressor instead of a down-ramp regressor. The areas on the left are the same results shown in Fig. 8, shown here for comparison. The results on the right are for the same analysis except using a boxcar instead of a down-ramp. That is, areas showing both a main effect of trial type (dots vs. arrows) and an interaction between trial type and regressor type (up-ramp vs. boxcar) in GLM parameter estimates. All of the same thresholding applies as before ($p<0.001$, cluster threshold=10, side and edge nearest neighbors, radiological view, with a five-slice gap between subsequent slices).

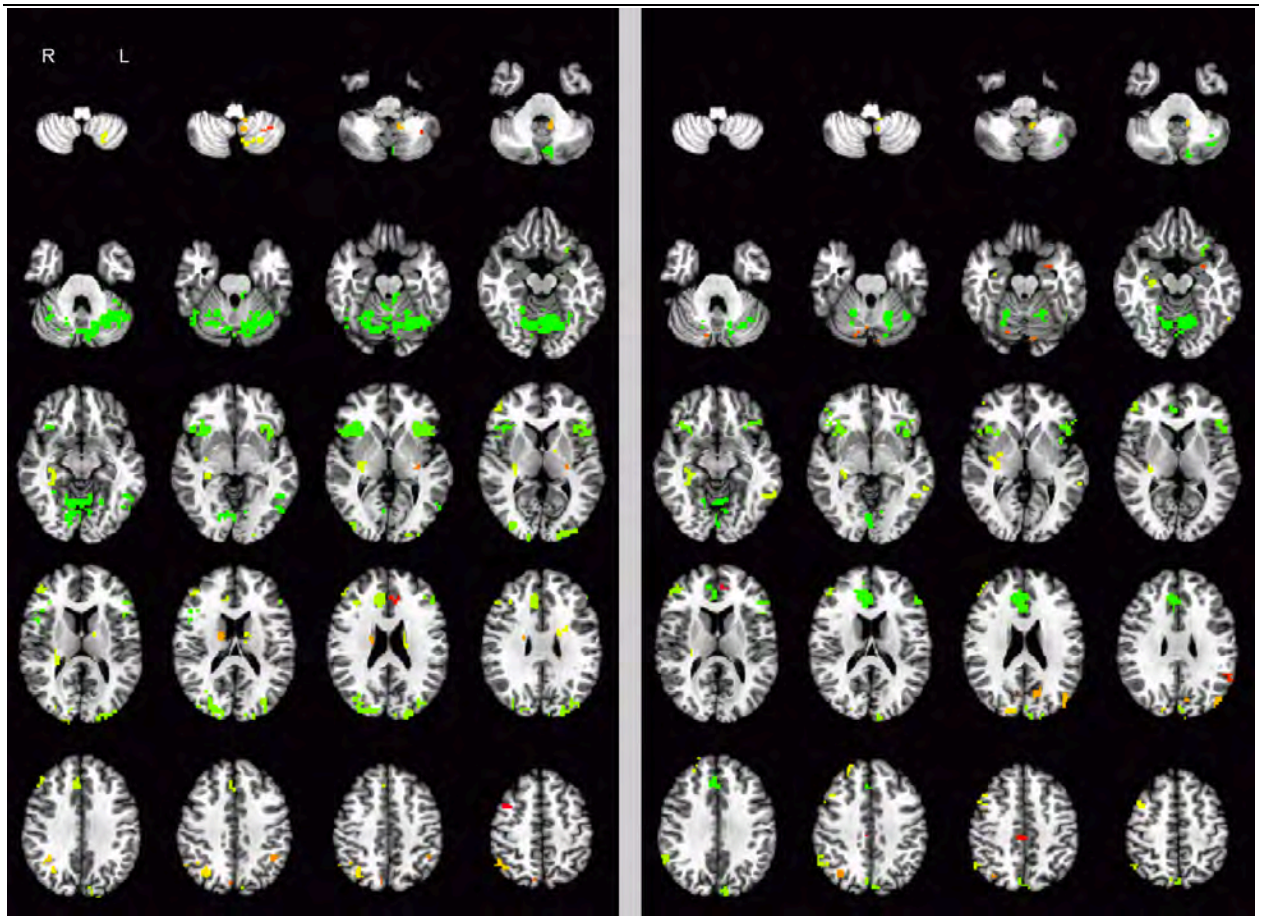

Fig. S7. Interaction between the dots/arrows condition and regressor type. The figure on the left uses the up-ramp and down-ramp as regressor types; the figure on the right uses up-ramp and a boxcar as regressor types. These two figures highlight the difference between using a down-ramp vs. a boxcar. The intersection of each of these figures with Fig. S2 (dots>arrows) produce the two figures in Fig. S6, respectively. The same thresholding is used, as before.

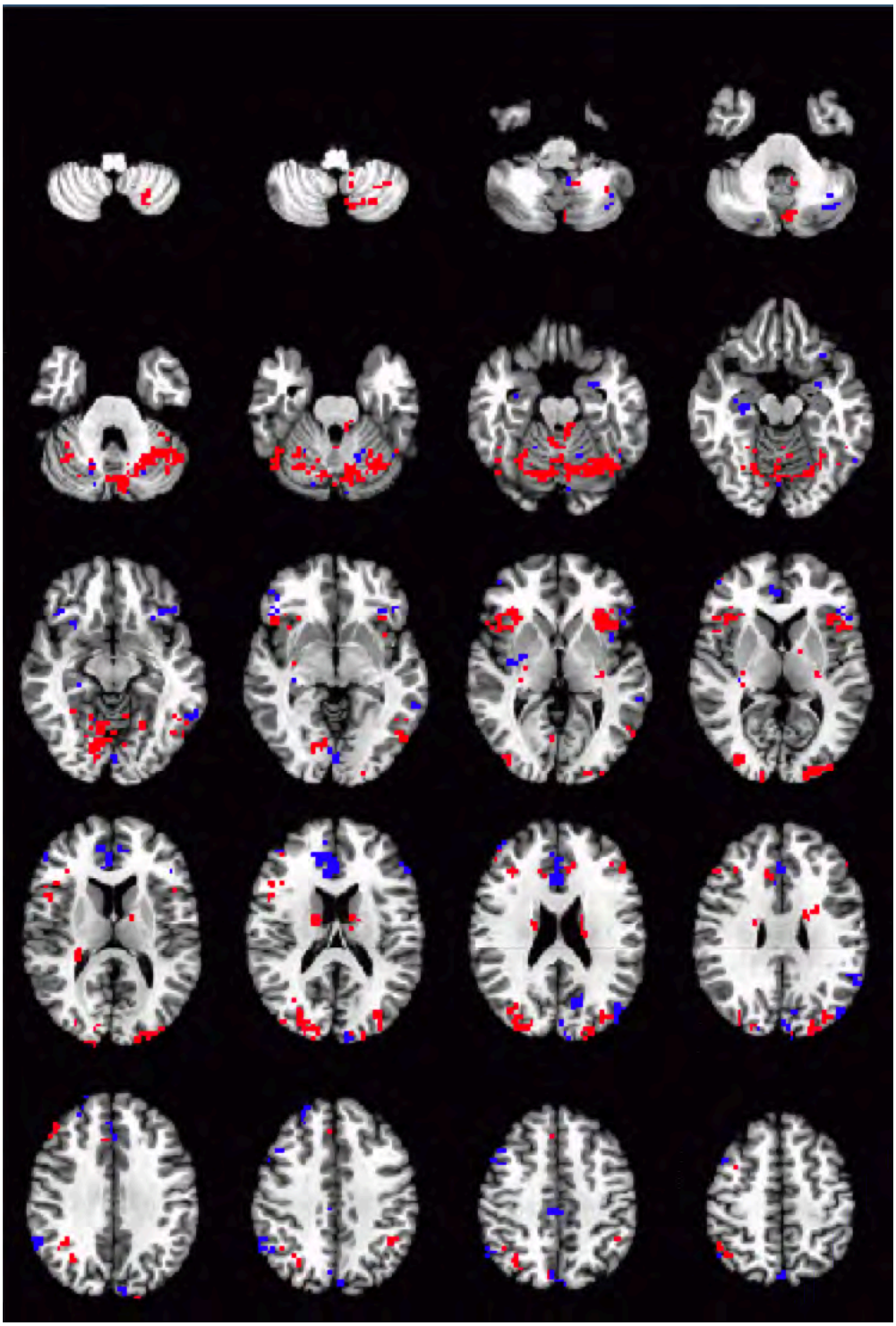

Fig S8. The difference between the masks of the two figures in Fig. S7: red indicates significant activation when using the down-ramp regressor but not when using the boxcar regressor; blue indicates significant activation when using the boxcar regressor but not when using the down-ramp regressor. The use of the down-ramp regressor detects an interaction between regressor type (up-ramp vs. down-ramp) and condition (dots vs. arrows) in several areas that are not detected when the down-ramp is replaced with a boxcar, including cerebellum, middle occipital gyrus, and insula. When using the boxcar, on the other hand, an interaction between regressor type (up-ramp vs. boxcar) and condition (dots vs. arrows) is found in some places that are not detected when using a down-ramp, most notably medial frontal cortex. The same thresholding is used as in previous figures.